



Enhancement of Saharan groundwater quality by reducing its fluoride concentration using different materials

Amina Ramdani^a, Safia Taleb^{a,*}, Abderazzak Benghalem^a, André Deratani^b,
Noreddine Ghaffour^c

^aLaboratory of Materials & Catalysis, Faculty of Sciences, Djillali Liabès University, Site I, B.P. 89, Sidi Bel-Abbès 22000, Algeria, Tel. +213 771218808; Fax: +213 48540360; email: safiatat@yahoo.fr

^bIEMIUM2, Place Eugène Bataillon, Case Courrier 047, 34095 Montpellier Cedex 5, France

^cWater Desalination & Reuse Centre, King Abdullah University of Science and Technology (KAUST), Djedjah, Saudi Arabia

Received 27 September 2013; Accepted 29 March 2014

ABSTRACT

According to the environmental protection regulations, fluoride concentration is considered as a substance of priority for assessment of drinking water quality to determine their impacts on the environment and public health. Saharan groundwater (Algeria) contains an excess of fluoride ions. Regular consumption of this water by the population of the region may cause endemic fluorosis. To solve this problem, we propose to treat this water by adsorption on different materials, such as activated alumina (AA), sodium clay (SC), and hydroxyapatite (HAP) in order to enhance its quality by reducing its fluoride concentration. The maximum adsorption is achieved with an adsorption capacity of the order of 0.9, 0.667, and 0.370 mg/g and with a percentage of 90, 83.4, and 73.95% for AA, HAP, and SC, respectively. Indeed, the acidity and alkalinity of the medium significantly affect the adsorption of fluoride ions. Results deduced from the curves of adsorption isotherms of fluoride ions showed that the retention is predictable from these isotherms in agreement with the Langmuir model. The low removal of fluoride ions was observed in presence of SO_4^{2-} , CO_3^{2-} , and HCO_3^- ions. Finally, AA material proved to be the best adsorbent for fluoride ions removal.

Keywords: Fluoride removal; Activated alumina; Sodium clay; Hydroxyapatite; Defluoridation

1. Introduction

Groundwater of the southeast region of Algeria (Sahara region) contains high levels of fluoride concentrations that often exceed the limits recommended by the World Health Organization (1.5 mg/L) [1]. Excess ingestion of fluoride can cause dental/skeletal fluorosis [2] affecting the health of people living in the

Sahara region, including El-Oued Souf where the percentage of this disease exceeds 80% [3]. Fluoride, as a contaminant in ground/surface water, could be from either natural geological sources or industrial wastes that use fluoride-containing compounds as raw materials [4–7]. Several studies have been conducted to estimate the concentration of fluoride ions present in drinking water, fruits, and vegetables [8].

*Corresponding author.

The current methods used to remove fluoride from water can be divided into several categories: chemical processes: precipitation [9], conventional physicochemical processes such as adsorption [10–18], electrocoagulation [19], ion exchange [20], and membrane processes: reverse osmosis [21–23], nanofiltration [21,24,25], and electrodialysis [26,27]. However, it is widely recognized that adsorption is an ideal and a suitable technique compared to other conventional techniques for water defluoridation for small communities [28]. Activated carbon has been for a long time the most effective adsorbent. Nevertheless, its major disadvantage is the high cost [10], which has led many researchers to develop their activities in investigating different low-cost and most effective materials [29], such as volcanic ash, natural or synthetic hydroxyapatite, activated alumina (AA), and especially clays which are known for their abundance in nature, in order to enhance the fluoride-removal performance. Moreover, the multiple physicochemical properties of these materials make them suitable for various applications.

Ku and Chiou [30] also studied the effect of some operational parameters on fluoride removal from aqueous solution by alumina. The removal efficiency was influenced significantly by the solution pH. The maximum fluoride removal (16.3 mg/g) was found at operating pH in the range of 5–7. Ghorai and Pant [31] conducted the sorption of fluoride by granulated AA. The removal of fluoride was maximized (69.5%) at pH 7 and was independent of the sorbent dose and initial fluoride concentration. The Langmuir maximum sorption capacity was found to be 2.41 mg/g.

In another investigation focused on chemical modification of bentonite clay using magnesium chloride in order to enhance its fluoride removal capacity [32], the magnesium-incorporated bentonite (MB) showed significantly high fluoride removal efficiency over a wide range of pH (3–10). Bicarbonate affected the fluoride removal significantly whereas other co-existing anions had no major effect on fluoride removal efficiency of MB. The prepared adsorbent showed a maximum fluoride removal capacity of 2.26 mg/g at an initial fluoride concentration of 5 mg/L, which was reported better than the unmodified bentonite.

Fluoride removal by montmorillonite clay has also been evaluated by Karthikeyan et al. [33]. Fluoride uptake was found maximum at pH 2, and decreased with an increase in pH solution. The material with particle size of 75 μm exhibited maximum percentage of fluoride adsorption compared to the other particle sizes. The Langmuir maximum sorption capacity for fluoride was found to be in the range of 1.485–1.910 mg/g at different temperatures. Fluoride

removal was found to be poorly affected only in the presence of HCO_3^- .

Sujana et al. [34] conducted defluoridation studies using amorphous iron and aluminum hydroxides with different molar ratios. The optimum pH for fluoride adsorption was found in the range of 4–5 for the oxide sorbents having molar ratios of 1:0, 3:1, and 2:1, whereas it was in the range of 4–7.5 for ratios of 1:1 and 0:1, and was attributed to both specific and non-specific adsorption on the sorbent surfaces. All samples exhibited high Langmuir adsorption capacities and the oxide adsorbent with molar ratio of 1 showed a maximum adsorption capacity of 91.7 mg/g. Adsorption and desorption studies have also been conducted to gain an insight into the adsorption mechanism on Fe/Al hydroxides surface by Sujana and Anand [35].

Extensive research has also been carried out for the removal of fluoride using various calcium salts as calcium has a good affinity for fluoride anion. Turner et al. [36] conducted fluoride removal studies using crushed limestone (99% pure calcite) by batch studies and surface-sensitive techniques from solutions with high fluoride concentrations ranging from 3 to 2.100 mg/L.

In the present study, we propose to use and compare the performance of different adsorbent materials such as AA, sodium clay (SC), and hydroxyapatite (HAP) in removing the excess fluoride from the Algerian Sahara groundwater (El-Oued Souf region). The objective of this research is to study and estimate their potential use as an adsorbent of fluoride ions, as well as the effect of the contact time, initial concentration, adsorbent dose, and pH of the solution.

2. Materials and methods

2.1. Materials

The raw clay (RC) used in this study is a natural montmorillonite collected from ENOF (National Company of the Non-ferrous Mining Products), Hammam Boughrara, Maghnia, located in the West of Algeria. AA and HAP are commercially available products. For the purification and the chemical activation of the clay used, we started by a RC sedimentation procedure to eliminate the quartz and cristobalite. With this process, the fraction montmorillonite ($<2 \mu\text{m}$) is obtained. The second step was the chemical activation which is based on the treatment of clay with hydrochloric acid (1 N) to remove carbonates, and by hydrogen peroxide to remove the organic components. The recovered solid phase was then saturated with sodium ions by stirring in sodium chloride solution (1 M). The obtained product (solid) is noted (SC).

2.2. Fluoride analysis

Fluoride was analyzed using a combination of the fluoride-specific electrode ELIT 8221 and the reference electrode 001 ELIT N (calomel), which was connected to a potentiometer (CyberScan pH/Ion 510). The meter was calibrated using 10 sodium fluoride solutions with concentrations ranging 0.1–10 mg/L, a range in which the electrode exhibits a true Nernstian behavior. Before any measurements were carried out, aliquots of 10 mL experimental solutions were mixed with 10 mL of total ionic strength adjusting buffer. The buffer was made to have concentrations of 58 g/L sodium chloride, 57 mL/L glacial acetic acid, 0.3 g/L trisodium citrate, and the pH was adjusted between 5 and 5.5 using sodium hydroxide [37–39]. The concentration of fluoride was measured after 5 min. Standard samples collected from water supply network of El-Oued Souf (Elrobbah) are set as a reference. The physicochemical analysis of water samples are presented in Table 1.

2.3. Characterization methods

AA, SC, and HAP materials were characterized by an Analytical Philips X'Pert Pro diffractometer operating at a wavelength $K\alpha$ of copper ($\lambda = 1.5418$) under a voltage of 45 kV and a current of 40 mA. The X-ray diffraction (XRD) was used to determine the crystalline phases present in these adsorbents. Surface area of the samples was measured by nitrogen adsorption–desorption method at 77 K and evaluated by the single point BET (Brunauer, Emmett, and Teller) method on a Micromeritics apparatus, Model 2100E. Analyzed samples were pretreated under vacuum (10^{-4} torr) at 150 °C for 1 h. Diffractograms of the different samples are presented in Figs. 1–3.

Table 1
Characteristics of water samples before and after treatment

Physicochemical parameters	Raw water	AA	HAP	SC
Conductivity, $\mu\text{S}/\text{cm}$	3,690	3,522	3,540	3,608
pH	7.43	7.54	7.52	7.48
Ca^{2+} , ppm	252	236	238.8	224
Mg^{2+} , ppm	123.93	118	120.1	109.6
Na^+ , ppm	338	306	310	292
K^+ , ppm	18	15	16.8	10.6
Cl^- , ppm	905.25	871.9	878.6	905.65
F^- , ppm	2.5	0.54	0.692	1.115
SO_4^{2-} , ppm	594.61	576	572.8	594.4
HCO_3^- , ppm	244	233.5	234	239.6

2.4. Batch adsorption studies

Adsorption experiments were performed by agitating a specific quantity of adsorbent (AA, SC, and HAP) with 100 mL of synthetic solutions with desired concentrations of fluoride in different flasks in a shaking thermostat bath at selected temperatures. After stabilization (equilibrium), the sorbate is filtered and analyzed.

Adsorption equilibrium studies were conducted by varying: the initial fluoride concentration, 2–8 mg/L; contact time solid–liquid, 5–120 min; adsorbent dose, 1–10 g/L; pH, 2–10; and Cl^- , SO_4^{2-} , CO_3^{2-} , and HCO_3^- ions. The amount of fluoride adsorbed q_e (mg/g) was calculated using the following equation:

$$q_e = \frac{X}{m} = \frac{(C_i - C_{\text{eq}})V}{m} \quad (1)$$

where C_i is the initial concentration (mol/L), C_{eq} is the equilibrium concentration (mol/L), V is the volume of the solution (L), m is the mass of adsorbent used (g), and X is the number of grams of fluorides adsorbed (mg).

The percentage adsorption (%) is calculated using the equation:

$$\% \text{ Adsorption} = \frac{(C_i - C_{\text{eq}}) 100}{C_i} \quad (2)$$

3. Results and discussion

3.1. Characterization

XRD spectra presented in Fig. 1 show that the impurities are widely removed during the purification process. However, the disappearance of certain lines related to the crystalline impurities $2\theta = 9^\circ$, 26.5° , and 29° correspond to illite (10 Å), quartz (3.34 Å), and

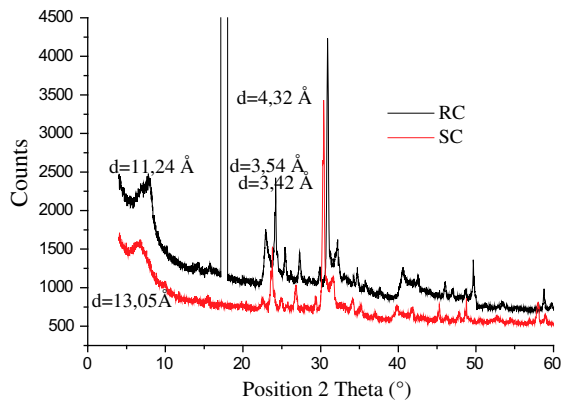


Fig. 1. Diffractograms of RC and SC samples.

Felds paths and calcite (3.03 \AA), respectively. The intensified crystalline of the montmorillonite peak (14 \AA) at $2\theta = 6.75^\circ$ confirms the good purification of SC.

On the basis of spectral data presented in Fig. 2, examination of the X-ray diffractogram of the AA indicates that the peaks of the diffraction patterns show the presence of crystalline phases mainly as bayerite, gibbsite, and nordstrandite [40]. Bayerite is the main component here, and gibbsite and nordstrandite are probably present too. The crystallographic peaks at $2\theta = 18.25^\circ, 19.4^\circ, 32.2^\circ, 37.49^\circ, 39.5^\circ, 42.6^\circ, 45.8^\circ,$ and 67.12° , correspond to the distances 4.85, 4.92, 2.78, 2.37, 2.28, 2.12, 1.98, and 1.39 \AA , respectively. Furthermore, we observe that the peak found at $2\theta = 45.8^\circ$ corresponds to the AA, $\gamma\text{-Al}_2\text{O}_3$; these results are consistent with previous studies [41]. The XRD of the HAP is presented in Fig. 3. The crystallographic peaks at $2\theta = 25.9^\circ, 32^\circ, 32.6^\circ, 33^\circ, 35.5^\circ,$ and 40° corresponding to the lattice planes (200), (211), (112), (300), (202), and (310), respectively, confirm the formation of the HAP structure [42,43].

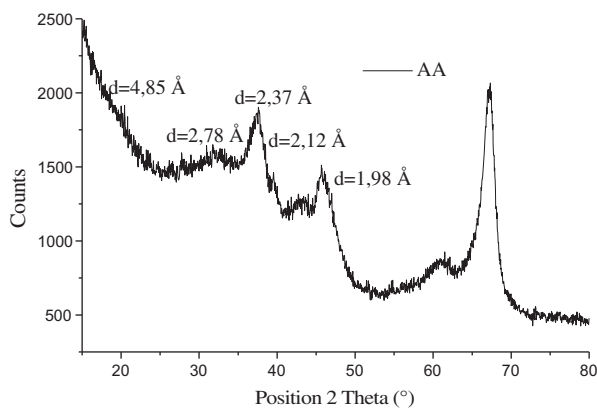


Fig. 2. Diffractograms of AA samples.

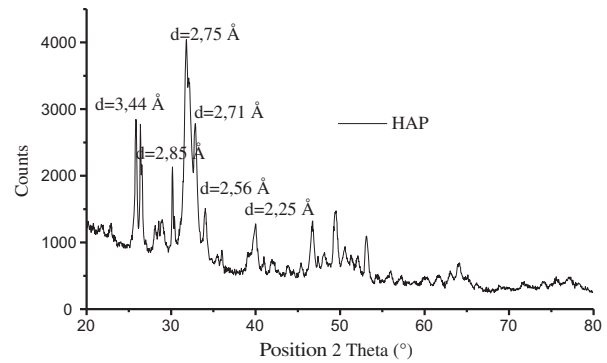


Fig. 3. Diffractograms of HAP samples.

The specific surface area of the purified clay and RC is 96 and $42 \text{ m}^2/\text{g}$, respectively. Moreover, results obtained for AA and HAP showed that the specific surface area is quite large compared to SC ($250 \text{ m}^2/\text{g}$).

3.2. Effect of contact time and initial concentration

Figs. 4–6 show the kinetics of adsorption of fluoride at various initial concentrations carried out using AA, SC, and HAP as adsorbents. It is obvious that the adsorption of fluoride onto AA is much faster than that of HAP and SC at the initial period of time, which suggests that the time required for a complete adsorption, 45 min of stirring, is sufficient to reach equilibrium, and then it stabilizes after 60 min.

It was observed that the adsorption capacity of the adsorbent increases from 0.9 to 2.675 mg/g , from 0.694 to 1.5 and from 0.37 to 0.656 for AA, HAP, and SC, respectively, when the initial concentration increases from 2 to 8 mg/L . Indeed, at low initial concentrations, the adsorption equilibrium is quickly reached and saturation is achieved; while with high initial concentrations, the adsorption is slow and

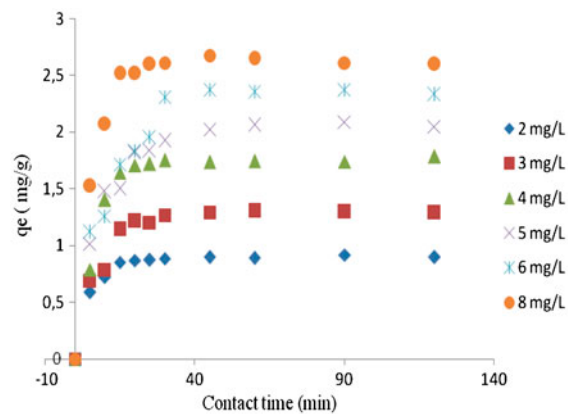


Fig. 4. Adsorption kinetics of fluoride ions on AA.

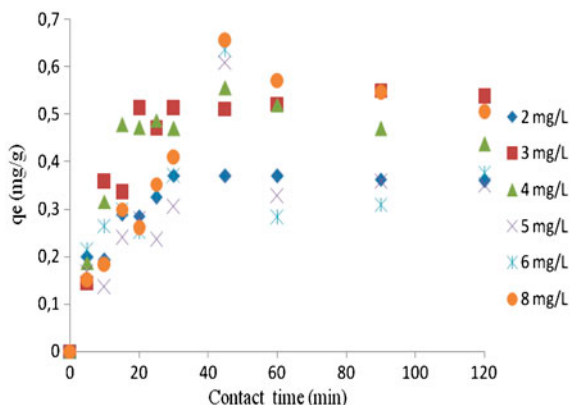


Fig. 5. Adsorption kinetics of fluoride ions on SC.

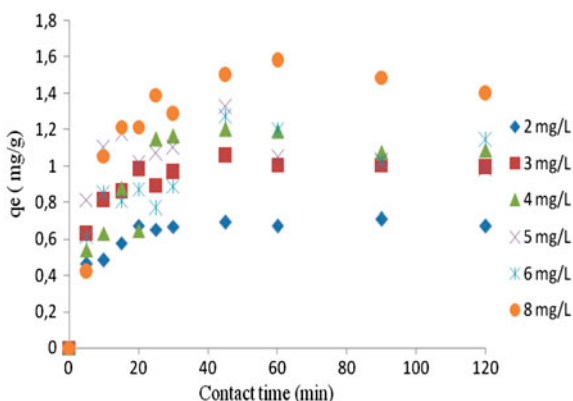


Fig. 6. Adsorption kinetics of fluoride ions on HAP.

saturation is not reached. Furthermore, the maximum adsorption is achieved with an adsorption capacity of the order of 0.9, 0.667, and 0.370 mg/g and with a percentage of 90, 83.4, and 73.95% for AA, HAP, and SC, respectively, for an initial concentration of 2 mg/L.

3.3. Effect of adsorbent dose

Effect of the variation of the adsorbent dose on the residual fluoride concentration from aqueous solution with AA, HAP, and SC used in this study is presented in Fig. 7. The figure clearly shows that a significant fluoride removal was achieved at a minimum dose of 2 g/L for AA, 2.5 g/L for HAP and 4 g/L for SC. Obviously, the residual fluoride concentration decreases rapidly with the increase of adsorbent content for all adsorbents. An addition of adsorbent dose beyond this value did not cause any significant change in the adsorption capacity.

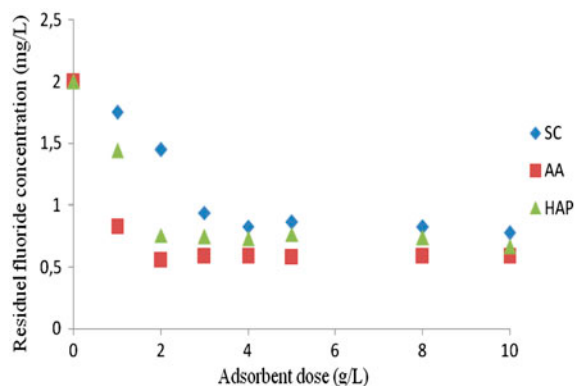


Fig. 7. Effect of adsorbent dose on residual fluoride concentration.

3.4. Effect of pH

The removal of fluoride ions from aqueous solution by adsorption is dependent on pH of the solution. A series of experiments with varying initial pH of the solution (from 2 to 10), by adding HCl (0.1 M) or NaOH (0.1 M) to adjust to the desired pH value, have also been conducted to determine the optimum pH range for maximum fluoride adsorption by the different adsorbents (AA, HAP, and SC). The graphical representation of the adsorption data of fluoride ions for the different adsorbents over the studied pH range is shown in Fig. 7. The maximum adsorption is reached at pH 4 for the AA and SC. Moreover, the adsorption of HAP increases with pH up to pH 3. Hence, the defluoridation capacity of the adsorbent is effective in acidic range. This can be explained due to the change in surface charge of the adsorbent. This is attributed to a greater increase in the attractive force between positively charged surface and negatively charged fluoride ions [44]. On the other hand, at high pH there is a sharp drop in adsorption, which is due to the negative charge of the materials surface. It can be concluded that the fluoride adsorption is explained by anion exchange. In addition, ion exchange mechanism is also involved in fluoride removal by AA, SC, and HAP. The OH group present in these adsorbents is considered as the charge carrier and can get exchanged with F^- ions [28,45,46].

3.5. Establishment of adsorption isotherms

We compared the measured adsorption of fluoride to adsorbents, with values evaluated from Langmuir and Freundlich isotherms (Figs. 8 and 9). The most important model of a monolayer adsorption comes from of Langmuir's work [47]. However, the Freundlich model assumes a heterogeneous adsorption

surface and active sites with different energy. The linearized form of the Langmuir and Freundlich isotherms is given below.

$$\text{Langmuir model: } \frac{C_{eq}}{q_e} = \frac{1}{K_L q_m} + \frac{C_{eq}}{q_m} \quad (3)$$

$$\text{Freundlich model: } \log q_e = \log K_F + \frac{1}{n} C_{eq} \quad (4)$$

where q_m is the maximum amount adsorbed of the adsorbent (mg/g) and K_L , K_F , and n are constants for Langmuir and Freundlich models, which are presented in Table 2. The Langmuir model usually fitted better with the obtained experimental data rather than the Freundlich model since the R^2 correlation values of Langmuir were higher and exceed 0.975 for all adsorbents. This indicates the probable formation of a monolayer of fluoride without mutual interactions of localized sites whose energy is identical. Also, some other studies showed that Langmuir isotherms correspond well with the experimental results of de-fluoridation [45,46].

3.6. Adsorption kinetics

In order to investigate the sorption mechanism of fluoride removal onto AA, HAP, and SC adsorbents, pseudo-first-order, pseudo-second-order kinetic models [17,48], and the intra-particle diffusion model [48] have been used in this study. The application of the pseudo-second-order equation and the intra-particle diffusion model for the adsorption of different adsorbents on fluoride is shown in Figs. 11 and 12, respectively.

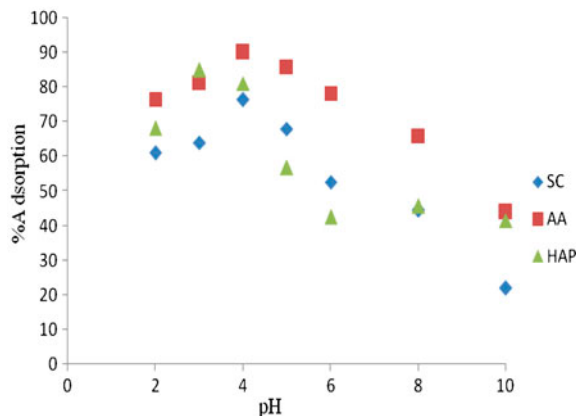


Fig. 8. Influence of pH on the adsorption of fluoride.

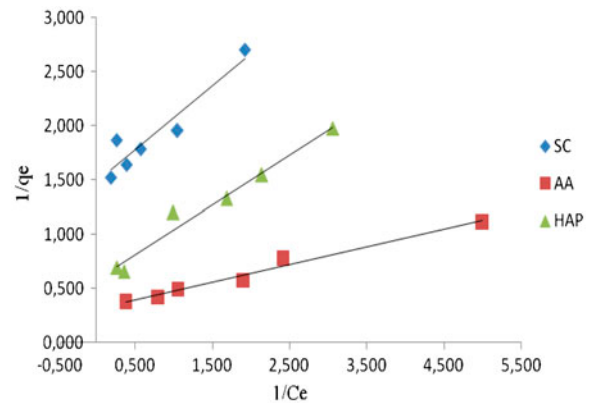


Fig. 9. Transformed linear Langmuir isotherms for adsorption of fluorides on different materials.

$$\log (q_e - q_t) = \log (q_e) - \left(\frac{k_1}{2.303} \right) t \quad (5)$$

$$\frac{t}{q_t} = \left(\frac{1}{k_2 q_e^2} \right) + \left(\frac{1}{q_e} \right) t \quad (6)$$

$$q_t = \frac{X}{m} = K_{diff} t^{1/2} \quad (7)$$

where q_t and q_e are the amount of adsorption at time t and at equilibrium (mg/g), respectively, k_1 is the constant rate of pseudo-first-order (1/min), k_2 is the constant rate of pseudo-second-order (g/(mg min)), and k_{diff} is the intra-particle diffusion coefficient (mg/(g min)).

The constant rates k_1 , k_2 , k_{diff} , and the amount of adsorption at equilibrium q_e were calculated from the slope and intercept of the corresponding linear lines, respectively. Results obtained by calculation using Eqs. ((5)–(7)) show that fluoride adsorption kinetics are well fitted by the pseudo-second-order model with an intra-particle diffusion since the obtained correlation coefficients were high (0.9–1.00) for all adsorbents.

3.7. Effect of interfering ions on the absorption of fluoride

Groundwater contains more anions that could influence the adsorption process to understand the effect of interfering ions. The adsorption studies were performed in the presence of sodium chloride, sodium sulfate, sodium carbonate, and sodium bicarbonate on the adsorption of fluoride ions with 2 mg/L as initial fluoride concentration, and a contact time of 45 min.

Table 2
Constants of Langmuir and Freundlich models

Sorbate	Sorbent	Langmuir			Freundlich		
		q_m (mg/g)	K_L (L/mg)	R^2	K_F (L/mg)	$1/n$	R^2
Fluorures	AA	3.213	1.908	0.98	1.981	2.313	0.93
	HAP	1.714	1.272	0.975	1.137	2.288	0.96
	SC	1.513	0.478	0.98	0.627	4.146	0.92

Concentrations of salts were varied from 100, 200, 300, 400, and 500 mg/L.

Results plotted in Figs. 10–12 show the effect of different concentrations of anions on the adsorption of fluoride ions from the aqueous solution. It was observed that there is no significant influence on AA, HAP, and SC materials in the presence of Cl^- . However, in the presence of HCO_3^- , the fluoride removal efficiency ranges between 54.8 and 81.6%, while in the presence of SO_4^{2-} and CO_3^{2-} , the percentage of fluoride removal decreases with the increasing concentration of sulfates and carbonates. This indicates the reduced removal of fluoride ions observed in the presence of SO_4^{2-} , CO_3^{2-} , and HCO_3^- ; hence from the above discussion it can be concluded that these anions will compete with fluoride ions during sorption of the active surfaces on the adsorbent. Similar results were obtained for the adsorption of fluoride in aqueous solution using AA, HAP, and montmorillonite clay [28,33,46,49].

3.8. Application of adsorption to natural water

(Figs. 13–15) After the experiments with synthetic solutions, the removal of fluoride ions by means of

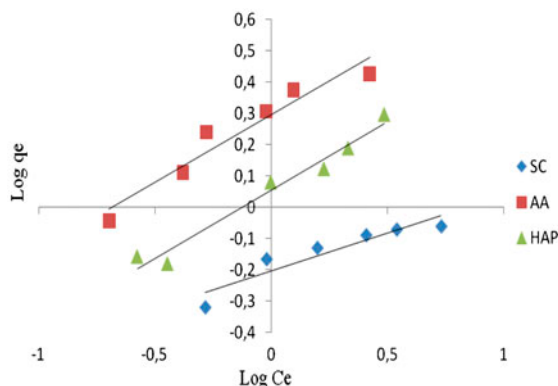


Fig. 10. Transformed linear Freundlich isotherms for adsorption of fluorides on different materials.

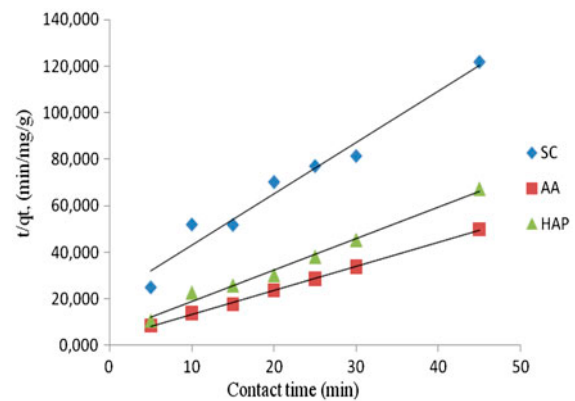


Fig. 11. Pseudo-second order for the adsorption of fluoride on different adsorbents.

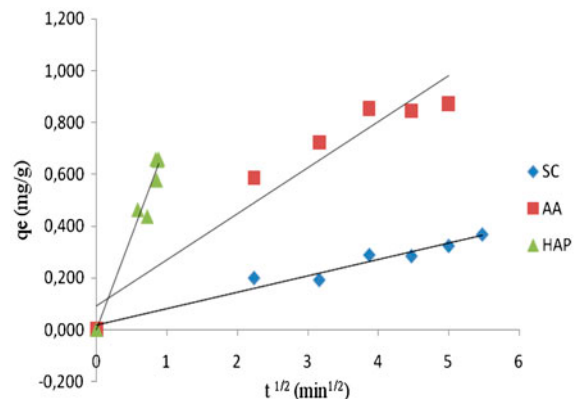


Fig. 12. Intra-particle diffusion for the adsorption of fluoride on different adsorbents.

adsorption by AA, HAP, and SC materials is subjected to Saharan groundwater collected from wells and consumer tap. It appears from the results that the optimal retention of fluoride ions which determine the standards for drinking water is obtained at a time longer than that obtained in the case of synthetic water. This

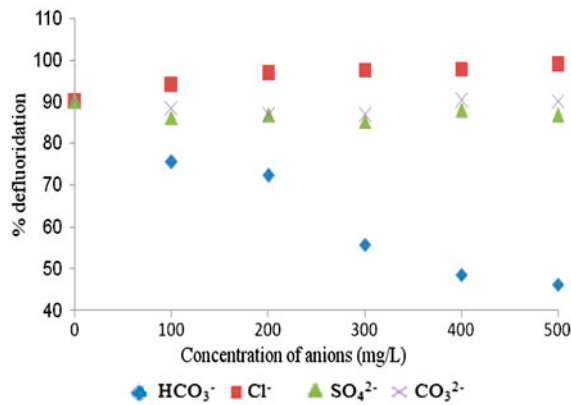


Fig. 13. Effect of interfering ions on the adsorption of fluoride by AA.

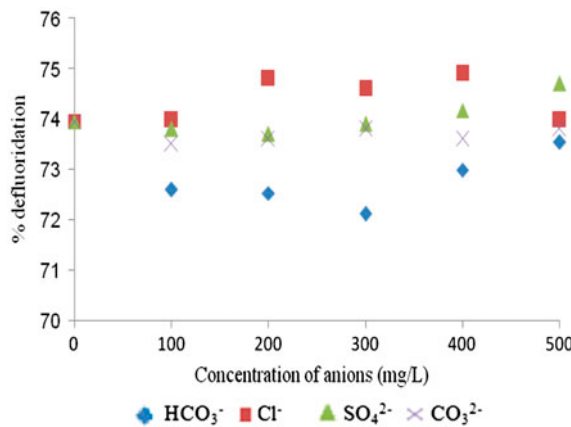


Fig. 14. Effect of interfering ions on the adsorption of fluoride by SC.

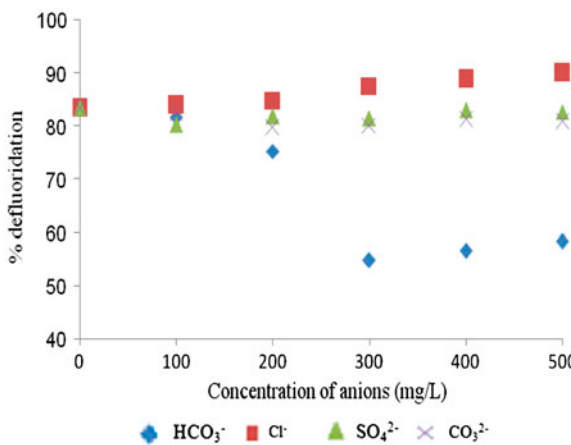


Fig. 15. Effect of interfering ions on the adsorption of fluoride by HAP.

explains the coexistence of HCO₃⁻ and SO₄²⁻ anions, which reduce the retention of fluoride ions.

4. Conclusions

Three different adsorbent materials (AA, SC, and HAP) have been investigated in this study aiming to enhance Saharan groundwater quality by reducing its high fluoride concentration. The adsorption rate of AA was found to be faster compared to that of HAP and SC, and the equilibrium time for fluoride removal is 60 min. The acidity of the medium significantly affects the adsorption of fluoride ions. At low initial concentrations, the adsorption equilibrium is quickly reached and saturation is achieved; while at high initial concentrations, the adsorption was slow and saturation was not reached. Fluoride removal has been achieved at a minimum dose of 2 g/L for AA, 2.5 g/L for HAP, and 4 g/L for SC. The best-fitting adsorption isotherm was the Langmuir isotherm, while the pseudo-second-order model was the best choice to describe the fluoride adsorption behavior with intra-particle diffusion. Among the competing ions, sulfate, bicarbonate and carbonate have shown significant effect on fluoride removal by AA, HAP, and SC except chloride ions. Fluoride adsorption can be explained by anion exchange. On the other hand, AA proved to be a good adsorbent for fluoride ions; it can also be proposed to reduce the salinity of groundwater. Future work will be focused on investigating the possible regeneration of these adsorbent materials. Several studies have shown that these kinds of adsorbents are widely available at low cost. They, however, have remarkable adsorption capacity requiring frequent regeneration [11,49–51].

Nomenclature

- AA — activated alumina
- C_{eq} — equilibrium concentration (mol/L)
- C_i — initial concentration (mol/L)
- HAP — hydroxyapatite
- q_e — amount of fluoride adsorbed at equilibrium (mg/g)
- q_t — amount of fluoride adsorbed at time *t* (mg/g)
- q_m — maximum adsorption capacity (mg/g)
- k₁ — constant rate of pseudo-first-order (1/min)
- k₂ — constant rate of pseudo-second-order (g/(mg min))
- k_{diff} — intra-particle diffusion coefficient (mg/(g min))
- m* — mass of the adsorbent (g)
- RC — raw clay
- SC — sodium clay
- V* — volume of the solution (L)
- X* — number of grams of fluoride adsorbed (mg)

References

- [1] World Health Organization (WHO), Fluoride in Drinking Water, WHO Guidelines for Drinking Water Quality, 2004, Available from: http://www.who.int/water_sanitation_health/dwq/gdwq3rev/en/.
- [2] M. Mahramanlioglu, I. Kizilcikli, I.O. Bicer, Adsorption of fluoride from aqueous solution by acid treated spent bleaching earth, *J. Fluorine Chem.* 115 (2002) 41–47.
- [3] N. Mameri, A.R. Yeddou, H. Lounici, D. Belhocine, H. Grib, B. Bariou, Defluoridation of septentrional Sahara water of North Africa by electrocoagulation process using bipolar aluminium electrodes, *Water Res.* 32 (1998) 1604–1612.
- [4] Y. Wang, E.J. Reardon, Activation and regeneration of a soil sorbent for defluoridation of drinking water, *Appl. Geochem.* 16 (2001) 531–539.
- [5] Y. Çengeloglu, E. KÝr, M. Ersöz, Removal of fluoride from aqueous solution by using red mud, *Sep. Purif. Technol.* 28 (2002) 81–86.
- [6] H. Wang, J. Chen, Y. Cai, J. Ji, L. Liu, H.H. Teng, Defluoridation of drinking water by Mg/Al hydrotalcite-like compounds and their calcined products, *Appl. Clay Sci.* 35 (2007) 59–66.
- [7] N. Drouiche, H. Lounici, M. Drouiche, N. Mameri, N. Ghaffour, Removal of fluoride from photovoltaic wastewater by electrocoagulation and products characteristics, *Desalin. Water Treat.* 7 (2009) 236–241.
- [8] S. Achour, La qualité des eaux du Sahara Septentrional en Algérie: Etude de l'excès du fluor [The water quality of Algerian Northern Sahara: Study of the fluorine excess], *Tribu. EAU.* 42(542) (1990) 53–57.
- [9] C.J. Huang, J.C. Liu, Precipitate flotation of fluoride-containing wastewater from a semiconductor manufacturer, *Water Res.* 33 (1999) 3403–3412.
- [10] A. Bhatnagar, E. Kumar, M. Sillanpää, Fluoride removal from water by adsorption – A review, *Chem. Eng. J.* 171 (2011) 811–840.
- [11] A. Tor, Removal of fluoride from an aqueous solution by using montmorillonite, *Desalination* 201 (2006) 267–276.
- [12] Y. Ma, F. Shi, X. Zheng, J. Ma, C. Gao, Removal of fluoride from aqueous solution using granular acid-treated bentonite (GHB): Batch and column studies, *J. Hazard Mater.* 185 (2011) 1073–1080.
- [13] T. Wajima, Y. Umeta, S. Narita, K. Sugawara, Adsorption behavior of fluoride ions using a titanium hydroxide-derived adsorbent, *Desalination* 249 (2009) 323–330.
- [14] M. Mourabet, A. El Rhilassi, H. El Boujaady, M. Bennani-Ziatni, R. El Hamri, A. Taitai, Removal of fluoride from aqueous solution by adsorption on apatitic tricalcium phosphate using Box–Behnken design and desirability function, *Appl. Surf. Sci.* 258 (2012) 4402–4410.
- [15] W.X. Gong, J.H. Qu, R.P. Liu, H.C. Lan, Adsorption of fluoride onto different types of aluminas, *Chem. Eng. J.* 189–190 (2012) 126–133.
- [16] J.H. Kim, C.G. Lee, J.A. Park, J.K. Kang, N.C. Choi, S.B. Kim, Use of pyrophyllite clay for fluoride removal from aqueous solution, *Desalin. Water Treat.* 51 (2013) 3408–3416.
- [17] M. Mourabet, A. El Rhilassi, M. Bennani-Ziatni, R. El Hamri, A. Taitai, Studies on fluoride adsorption by apatitic tricalcium phosphate (ATCP) from aqueous solution, *Desalin. Water Treat.* 51 (2013) 6743–6754.
- [18] S.K. Swain, T. Patnaik, R.K. Dey, Efficient removal of fluoride using new composite material of biopolymer alginate entrapped mixed metal oxide nanomaterials, *Desalin. Water Treat.* 51 (2013) 4368–4378.
- [19] N. Drouiche, S. Aoudj, M. Hecini, N. Ghaffour, H. Lounici, N. Mameri, Study on the treatment of photovoltaic wastewater using electrocoagulation: Fluoride removal with aluminium electrodes – Characteristics of products, *J. Hazard. Mater.* 169 (2009) 65–69.
- [20] A. Tor, Removal of fluoride from water using anion-exchange membrane under Donnan dialysis condition, *J. Hazard. Mater.* 141 (2007) 814–818.
- [21] M. Pontié, H. Dach, J. Leparc, M. Hafsi, A. Lhassani, Novel approach combining physico-chemical characterizations and mass transfer modelling of nanofiltration and low pressure reverse osmosis membranes for brackish water desalination intensification, *Desalination* 221 (2008) 174–191.
- [22] W. Arras, N. Ghaffour, A. Hamou, Performance evaluation of BWRO desalination plant – A case study, *Desalination* 235 (2009) 170–178.
- [23] M. Pontie, H. Dach, A. Lhassani, C.K. Diawara, Water defluoridation using nanofiltration vs. reverse osmosis: The first world unit, Thiadiaye (Senegal), *Desalin. Water Treat.* 51 (2013) 164–168.
- [24] M. Tahaikt, A. Ait Haddou, R. El Habbani, Z. Amor, F. Elhannouni, M. Taky, M. Kharif, A. Boughriba, M. Hafsi, A. Elmidaoui, Comparison of the performances of three commercial membranes in fluoride removal by nanofiltration continuous operations, *Desalination* 225 (2008) 209–219.
- [25] J. Hoinkis, S. Valero-Freitag, M.P. Caporgno, C. Pätzold, Removal of nitrate and fluoride by nanofiltration – A comparative study, *Desalin. Water Treat.* 30 (2011) 278–288.
- [26] M.A. Menkouchi Sahli, S. Annouar, M. Tahaikt, M. Mountadar, A. Soufiane, A. Elmidaoui, Fluoride removal for underground brackish water by adsorption on the natural chitosan and by electro-dialysis, *Desalination* 212 (2007) 37–45.
- [27] M. Arda, E. Orhan, O. Arar, M. Yuksel, N. Kabay, Removal of fluoride from geothermal water by electro-dialysis (ED), *Sep. Sci. Technol.* 44 (2009) 841–853.
- [28] M.M. Shihabudheen, S. Atulkumar, P. Ligy, Manganese-oxide-coated alumina: A promising sorbent for defluoridation of water, *Water Res.* 40 (2006) 3497–3506.
- [29] D. Mohapatra, D. Mishra, S.P. Mishra, G.R. Chaudhury, R.P. Das, Use of oxide minerals to abate fluoride from water, *J. Colloid Interface Sci.* 275(2) (2004) 355–359.
- [30] Y. Ku, H.M. Chiou, The adsorption of fluoride ion from aqueous solution by activated alumina, *Water Air Soil Pollut.* 133 (2002) 349–361.
- [31] S. Ghorai, K.K. Pant, Equilibrium, kinetics and breakthrough studies for adsorption of fluoride on activated alumina, *Sep. Purif. Technol.* 42 (2005) 265–271.
- [32] D. Thakre, S. Rayalu, R. Kawade, S. Meshram, J. Subrt, N. Labhsetwar, Magnesium incorporated bentonite clay for defluoridation of drinking water, *J. Hazard. Mater.* 180 (2010) 122–130.

- [33] G. Karthikeyan, A. Pius, G. Alagumuthu, Fluoride adsorption studies of montmorillonite clay, *Indian J. Chem. Technol.* 12 (2005) 263–272.
- [34] M.G. Sujana, G. Soma, N. Vasumathi, S. Anand, Studies on fluoride adsorption capacities of amorphous Fe/Al mixed hydroxides from aqueous solutions, *J. Fluorine Chem.* 130 (2009) 749–754.
- [35] M.G. Sujana, S. Anand, Iron and aluminium based mixed hydroxides: A novel sorbent for fluoride removal from aqueous solutions, *Appl. Surf. Sci.* 256 (2010) 6956–6962.
- [36] B.D. Turner, P. Binning, S.L.S. Stipp, Fluoride removal by calcite: Evidence for fluorite precipitation and surface adsorption, *Environ. Sci. Technol.* 39 (2005) 9561–9568.
- [37] A. Tor, Removal of fluoride from an aqueous solution by using montmorillonite, *Desalination* 201 (2006) 267–276.
- [38] M. Agarwal, K. Rai, R. Shrivastav, S. Dass, Defluoridation of water using amended clay, *J. Clean. Prod.* 11 (2003) 439–444.
- [39] A. Ramdani, S. Taleb, A. Benghalem, Study of the optimization of the potential of adsorption of the local montmorillonite for the reduction of the excess of ions Fluorides of Saharan water, *Phys. Chem. News* 52 (2010) 89–97.
- [40] K.A. Rodgers, M.R. Gregory, R. Barton, Bayerite, nordstrandite, gibbsite, brucite, and pseudoboehmite in discharged caustic waste from Campbell Island, Southwest Pacific, *Clays. Clay Miner.* 39(1) (1991) 103–107.
- [41] M.M. Şovar, Du tri-isopropoxyde aux oxydes d'aluminium par dépôt chimique en phase vapeur: procédé, composition, et propriétés des revêtements obtenus [Of di-isopropoxyde to aluminum oxides by chemical deposit in phase vapor: Process, composition, and properties of the obtained covers], thèse de doctorat des Sciences et Génie des Matériaux [Ph.D thesis on Sciences and Engineering of Materials], l'institut national polytechnique de Toulouse, France, 2006.
- [42] M. Hadioui, Synthèse d'hydroxyapatite et de silice greffées pour l'élimination de métaux toxiques en solution aqueuses [Hydroxyapatite and silica grafted Synthesis for the toxic metals elimination in aqueous solution], thèse de doctorat [PhD thesis], Université Paul Sabatier de Toulouse III, France, 2007.
- [43] W. Jie, L. Yubao, Tissue engineering scaffold material of nano-apatite crystals and polyamide composite, *Eur. Poly. J.* 40 (2004) 509–515.
- [44] G. Karthikeyan, A. Shunmuga Sundarraj, S. Meenakshi, K.P. Elango, Adsorption dynamics and the effect of temperature of fluoride at alumina solution interface, *J. Indian Chem. Soc.* 81 (2004) 461–466.
- [45] A. Ramdani, S. Taleb, A. Benghalem, N. Ghaffour, Removal of excess fluoride ions from Saharan brackish water by adsorption on natural materials, *Desalination* 250 (2010) 408–413.
- [46] C.S. Sundaram, N. Viswanathan, S. Meenakshi, Defluoridation chemistry of synthetic hydroxyapatite at nano scale: Equilibrium and kinetic studies, *J. Hazard. Mater.* 155 (2008) 206–215.
- [47] O. Khazali, R. Abu-El-Halawa, K. Al-Sou'od, Removal of copper(II) from aqueous solution by Jordanian pottery materials, *J. Hazard. Mater.* 139 (2007) 67–71.
- [48] A. Ouldoumna, L. Reinert, N. Benderdouche, B. Bestani, L. Duclaux, Characterization and application of three novel biosorbents "*Eucalyptus globulus*, *Cynara cardunculus*, and *Prunus cerasifera*" to dye removal, *Desalin. Water Treat.* 51 (2013) 3527–3538.
- [49] S.P. Kamble, G. Deshpande, P.P. Barve, S. Rayalu, N.K. Labhsetwar, A. Malyshev, B.D. Kulkarni, Adsorption of fluoride from aqueous solution by alumina of alkoxide nature: Batch and continuous operation, *Desalination* 264 (2010) 15–23.
- [50] X. Wu, Y. Zhang, X. Dou, M. Yang, Fluoride removal performance of a novel Fe–Al–Ce trimetal oxide adsorbent, *Chemosphere* 69 (2007) 1758–1764.
- [51] V.S. Chauhan, P.K. Dwivedi, L. Iyengar, Investigations on activated alumina based domestic defluoridation units, *J. Hazard. Mater.* 139 (2007) 103–107.